Internal friction and absence of dilatancy of packings of frictionless polygons

Émilien Azéma, Farhang Radjaï, Jean-Noël Roux

PHYSICAL REVIEW E **91**, 010202(R) (2015)

Internal friction and absence of dilatancy of packings of frictionless polygons

Émilien Azéma,[1,*] Farhang Radjaï,[1,2,3,†] and Jean-Noël Roux[4,‡]

[1]*Université de Montpellier, CNRS, LMGC, Cc 048, Place Eugène Bataillon, F-34095 Montpellier cedex 05, France*

[2]*MIST, CNRS-IRSN, Université de Montpellier, France*

[3]*⟨MSE⟩², UMI 3466 CNRS-MIT, CEE, Massachusetts Institute of Technology, 77 Massachusetts Avenue, Cambridge, Massachusetts 02139, USA*

[4]*Université Paris-Est, Laboratoire Navier, 2 Allée Kepler, Cité Descartes, 77420 Champs-sur-Marne, France*

(Received 2 August 2014; published 30 January 2015)

By means of numerical simulations, we show that assemblies of frictionless rigid pentagons in slow shear flow possess an internal friction coefficient (equal to 0.183 ± 0.008 with our choice of moderately polydisperse grains) but no macroscopic dilatancy. In other words, despite side-side contacts tending to hinder relative particle rotations, the solid fraction under quasistatic shear coincides with that of isotropic random close packings of pentagonal particles. Properties of polygonal grains are thus similar to those of disks in that respect. We argue that continuous reshuffling of the force-bearing network leads to frequent collapsing events at the microscale, thereby causing the macroscopic dilatancy to vanish. Despite such rearrangements, the shear flow favors an anisotropic structure that is at the origin of the ability of the system to sustain shear stress.

DOI: 10.1103/PhysRevE.91.010202 PACS number(s): 45.70.Cc, 45.70.Mg

One of the most basic properties of slowly deformed solidlike granular materials is their *dilatancy*, i.e., their propensity to change volume under shear strain (or, more generally, deviatoric strain). In particular, initially dense granular assemblies will dilate under shear, and since its introduction by Reynolds in 1885 [1], this property is regarded as stemming from steric constraints [2], as one may expect from the naive image of Fig. 1, often relied upon in pedagogical documents.

In simple shear (see Fig. 1), with the convention that shrinking strains are positive, this property is conveniently expressed by dilatancy angle ψ, defined through the ratio of normal expansion rate $-\dot{\epsilon}_{yy}$ to shear rate $\dot{\gamma}$:

$$\tan\psi = \frac{-\dot{\epsilon}_{yy}}{\dot{\gamma}}. \tag{1}$$

This angle may be regarded as the kinematic dual of the friction angle φ or friction coefficient μ^*, defined as the ratio of shear stress to normal stress (coordinates are defined as in Fig. 1):

$$\mu^* = \tan\varphi = \frac{|\sigma_{xy}|}{\sigma_{yy}}. \tag{2}$$

An alternative definition of a friction angle φ relies on principal stresses $\sigma_1 > \sigma_2$, mean stress $p = (\sigma_1 + \sigma_2)/2$, and deviator $q = (\sigma_1 - \sigma_2)/2$:

$$\sin\varphi = \frac{q}{p}. \tag{3}$$

Definitions of φ in (2) and (3) coincide within the Mohr-Coulomb model (which does not exactly apply to granular materials [3]).

Dilatancy implies that the shear strength partly stems from the work against pressure that is necessarily spent in order to shear the granular material. The idea is often invoked to justify semiempirical *stress-dilatancy* relations [4] between φ and ψ, which numerical and micromechanical investigations [5–9] sought to support and to relate to internal state characteristics (such as fabric or force chains). In dense granular assemblies subjected to quasistatic shear under constant normal stress σ_{yy}, φ, as a function of growing shear strain γ, first increases to a maximum (the *peak deviator stress*, typically reached for strain γ_{peak} of the order of 10^{-2}), and then decreases to a final plateau (in the so-called *critical state* of soil mechanics [4]). Meanwhile, ψ, often negative in a small initial strain interval, increases to a positive maximum (reached near γ_{peak}), and then decreases until it vanishes, as the critical state is characterized by steady plastic flow at constant volume. Such a complex behavior is essentially determined, in the practically relevant limit of rigid undeformable grains, by packing geometry and contact sliding friction coefficient μ_s [10], with quite a significant effect of rolling friction too, if present [11,12]. How macroscopic rheological characteristics such as φ and ψ emerge as collective properties of disordered packings is by no means trivial.

In this context, assemblies of rigid particles with *frictionless* contacts are a particularly interesting limit case in which all mechanical properties are of purely geometric origin [13–20]. Moreover, if assembled under an isotropic state of stress, rigid frictionless grains stabilize with positions realizing a local minimum of volume in the configuration space [13,17], and as a consequence it is a common procedure to set $\mu_s = 0$ in numerical simulations in order to produce disordered packings of maximum density, for spheres [17,21], or other particle shapes, in two [22,23] and three dimensions [20,24–27]. Such frictionless isotropic packings have recently been studied for their specific, barely rigid structure [15,24], or simply used as convenient reference initial states [21–23], as they are relatively well reproducible and exhibit little dependence on assembling procedure [17]. Their structure is the one classically referred to as the *random close packing (RCP) state* [15–17].

Most often, in numerical simulation practice, such initial isotropic states are subjected to shear tests with a finite level

*emilien.azema@univ-montp2.fr
†franck.radjai@univ-montp2.fr
‡jean-noel.roux@ifsttar.fr

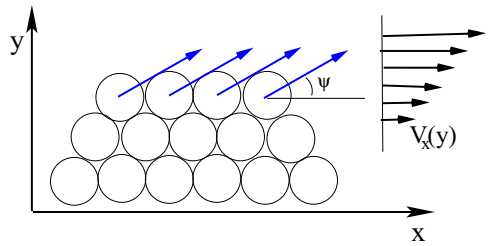

FIG. 1. (Color online) A classical representation of dilatancy mechanism in quasistatic simple shear test: Some expansion in direction y is necessary for adjacent layers to flow past one another.

of friction μ_s introduced in the contacts, which causes a strong dilatancy [6,21,23,28]. But different observations are made if spherical rigid grains are kept frictionless as the shear response is probed [19]. As the internal friction is (monotonically) growing with shear strain to its critical state value ($\varphi = 5.76 \pm 0.22^\circ$ [18,29]) no appreciable change in solid fraction is observed. The material is therefore constantly devoid of dilatancy ($\psi = 0$) [18,19]. The RCP density is thus observed in shear zones in frictionless bead assemblies [30]. Two-dimensional (2D) assemblies of frictionless rigid *disks* also exhibit a finite macroscopic friction angle [14,31], and various observations suggest that they are devoid of dilatancy (no clear-cut dilating or contracting tendency in [14], smaller and smaller dilatancy in the limit of $\mu_s \to 0$ in [6]). With frictionless spherical grains, or circular ones in 2D, no density change—no dilatancy—occurs while φ monotonically increases to its plateau value. Dilatancy angle ψ, for beads or disks, thus depends on contact friction coefficient μ_s, and vanishes for $\mu_s = 0$, rather unexpectedly, given that the simple picture of Fig. 1 ignores the role of intergranular friction.

We tested for the generality of such conclusions by investigating the internal friction and dilatancy properties of rigid, frictionless *angular* particles, in the simple case of a polydisperse collection of rigid pentagons in 2D. Unlike circular objects, any pair of polygons in side-to-side contact will exhibit some kind of "local dilatancy," causing their centers to move further apart, if a relative rotation occurs, as sketched in Fig. 2. A "local dilatancy" angle might thus be

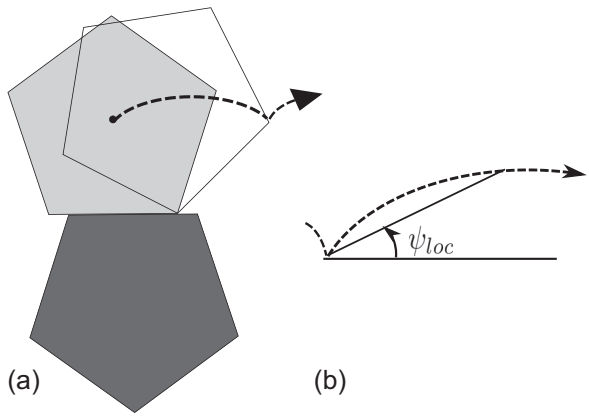

FIG. 2. (a) A polygon rolling on another polygon in side-to-side contact, whence (b) an effective dilatancy angle $\psi_{\rm loc}$.

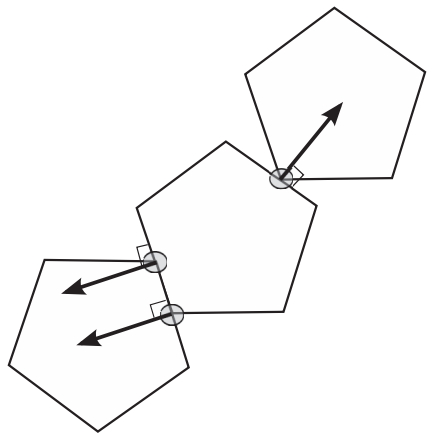

FIG. 3. A simple (vertex-side) contact and a double (side-side) one between polygonal grains, with corresponding normal forces.

identified as $\psi_{\rm loc} = \frac{\pi}{2n_s}$ in an assembly of regular polygons with n_s sides [32]. One might therefore wonder whether a macroscopic nonvanishing dilatancy angle ensues, and how the internal friction angle is affected by such angularity effects.

We addressed these issues by means of simulations using the *contact dynamics* (CD) method, which is suitably applicable to large assemblies of undeformable particles [10,33–35], in inertial flow [36], as well as in quasistatic evolution [7]. In this method, the rigid-body equations of motion are integrated and the kinematic constraints due to contacts are taken into account, using an implicit time-stepping scheme to simultaneously update the contact forces and the particle velocities. Contact interactions are characterized by three parameters: the coefficient of friction and the coefficients of normal and tangential restitution. The CD method has repeatedly been applied to the simulation of assemblies of angular grains, polygons in two dimensions [32,37] or polyhedra in three dimensions [27,38]. A small tolerance on grain overlaps enables contact detection (resulting in relative error on ν of order 10^{-4}), and polygons might interact by vertex-side or side-side contacts (vertex-vertex contacts are statistically irrelevant). A side-vertex contact is a "simple" contact, as between disks, and corresponds to a single unilateral constraint, with the normal direction orthogonal to the side (Fig. 3). A side-side contact is a "double" contact in the sense that it can be represented by two unilateral constraints. It is equivalent to two simple contacts between the same polygons, and the normal direction is the normal to their common side, as shown in Fig. 3. In practice, two forces are calculated at each side-side contact, but only the resulting total force and torque are physically meaningful [39].

The packings of frictionless pentagons or disks dealt with in the present study comprise 15 000 objects. Particle sizes are randomly chosen according to a uniform distribution in surface area, the diameter d of the circumscribed circle varying between $D_{\rm min}$ and $D_{\rm max} = 2D_{\rm min} = \langle d \rangle / \ln(2)$, $\langle d \rangle$ denoting the average value of d. First loosely arranged, with random orientations, in a laterally periodic (i.e., along the x axis) rectangular box, particles are then compressed between the smooth walls parallel to direction x. The normal restitution coefficient is equal to zero (no tangential forces or momentum

transfer exist in contacts, due to vanishing friction). In a second stage, both walls acquire some roughness as all pentagons with center at distance below $2\langle d\rangle$ are rigidly tied to them. A prescribed normal stress σ_{yy} is applied through those rough parallel walls. The solid fraction ν is evaluated in a bulk region, of thickness H, conventionally limited by the y coordinate of the centers of mass of both walls. Starting from either a loose initial configuration, or from an equilibrium state under the applied stress, shear flow is driven by moving the upper wall with prescribed velocity V_x, while the lower one remains immobile. The position (coordinate y) of the top wall, and thus the thickness H of the sheared layer, are free to fluctuate while stress σ_{yy} is maintained constant. V_x linearly increases in a first stage and is then maintained at a constant value. As in many previous studies of normal-stress controlled shear flow [18,31], shear stress σ_{xy} and solid fraction ν, after an initial transient (corresponding to strain $\gamma \simeq 0.2$), fluctuate about a steady state average value which depends on the *inertial number* [3,18,31,36], defined as $I = \frac{V_x}{H}\langle d\rangle\sqrt{\frac{\rho}{\sigma_{yy}}}$ (ρ is the mass density of the grains). I is the ratio of inertial time $\langle d\rangle\sqrt{\rho/\sigma_{yy}}$ to shear time H/V_x. It characterizes inertial effects, and vanishes in the quasistatic limit. All values of friction angles or coefficients indicated in the following pertain to the steady state. The averages of the time series provide estimates of macroscopic friction angle φ and solid fraction ν, which depend on I, as plotted in Fig. 4. Error bars are deduced from rms. variations about averages. The present study focuses on the quasistatic limit of $I \to 0$ (approached with good accuracy for $I \leqslant 10^{-4}$). Our measured value of q/p, $q/p = \sin\varphi = 0.183 \pm 0.008$, yields a larger friction angle, $\varphi = 10.5 \pm 0.4^\circ$ [40], for pentagons than for disks, in which case our result $q/p = 0.099 \pm 0.002$ corresponds to $\varphi = 5.7 \pm 0.15^\circ$. As to solid fractions, we estimate their quasistatic limits as $\nu = 0.854 \pm 0.003$ for pentagons, and $\nu = 0.8425 \pm 0.0008$ for disks. Our results for ν and φ in disk assemblies agree with previously published ones [12,31], despite the different diameter distributions.

For comparison, RCP configurations are assembled in separate simulations of isotropic compression tests, with the same number of particles, as in [41]. Bulk solid fractions equal to 0.8530 ± 0.0013 for pentagons, to 0.8433 ± 0.0003 for disks are then measured on correcting for wall effects and averaging over several samples. These values coincide, within statistical uncertainties, with the ones observed in the limit of slow steady shear flows. No significant density change, either, was observed in shear flow in the transient evolution between initial state and steady state (while the shear stress increases monotonically to its steady state value [42]). Hence the conclusion is that pentagons, like disks, are as densely packed in steady quasistatic shear flow as in the isotropic RCP state. Within statistical uncertainties, such assemblies of angular particles, just like packs of disks (or of spherical beads in three-dimensional [18,19]), despite the local dilatancy at contact scale (Fig. 2), are devoid of macroscopic dilatancy if contacts are frictionless.

Some insight on the origins of this discrepancy between microscopic and macroscopic dilatancy behaviors might be gained on investigating particle motions and local density changes. Packs of frictionless particles, in which stresses are barely supported by isostatic contact networks, are notoriously unstable and prone to collective rearrangements [14,19]. The effect of such events on the system volume fluctuate strongly in space (as apparent in Fig. 5) and in time, and average zero. Figure 5 illustrates the local volume changes around each polygon, identified on using a local measure proposed in [43] for strain rate $\underline{\underline{\dot{\epsilon}}}$. While the spatial average of its trace is of

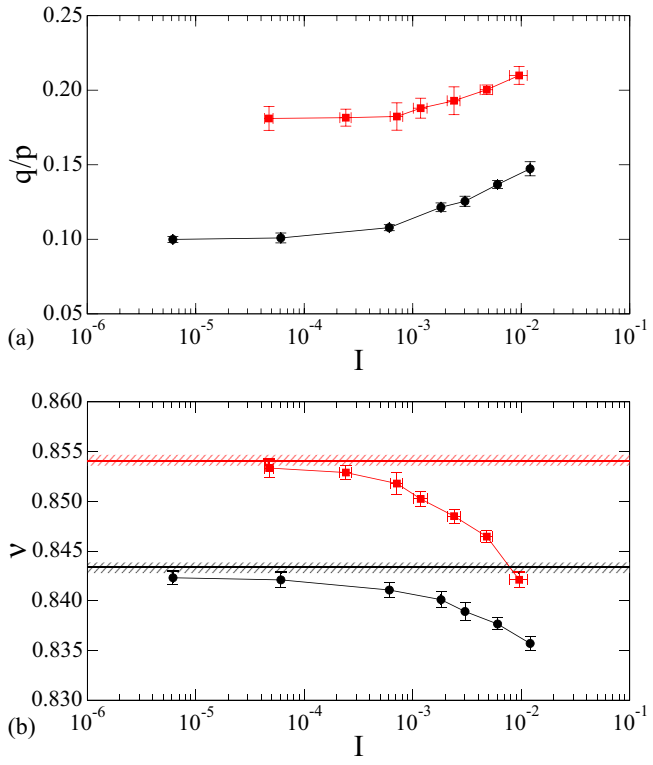

FIG. 4. (Color online) Steady shear flow results. (a) $\sin\varphi = q/p$ versus I, with(red) squares for pentagons and (black) dots for disks. (b) ν versus I (same symbols and colors). The horizontal straight line corresponds to isotropic equilibrium (RCP) values, hashed regions indicating the error bar.

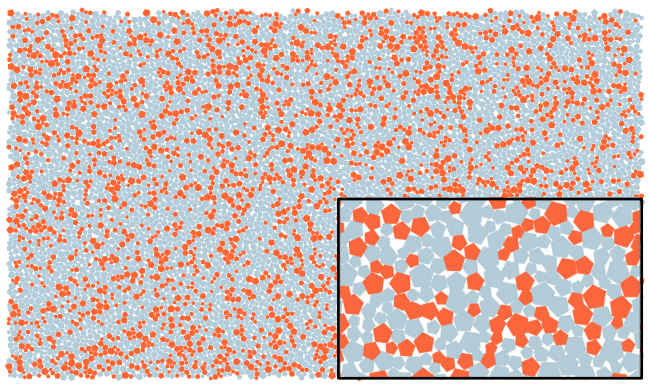

FIG. 5. (Color online) Each polygon is colored according to the sign of the local area change: orange (or darker gray) for a local dilation; light blue (or gray) for a local contraction. The inset shows a smaller scale detail.

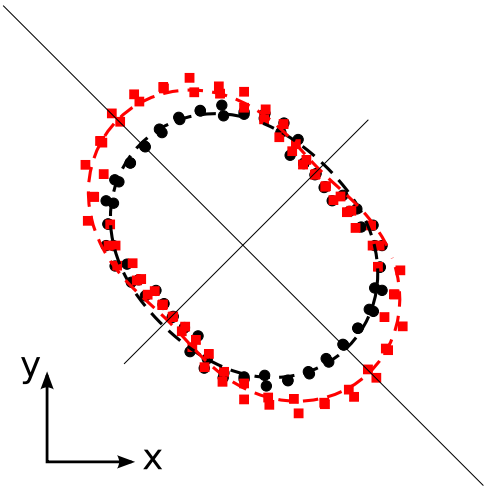

FIG. 6. (Color online) Polar diagrams of $P(\theta)$ (black dots) and $\langle f_n\rangle(\theta)$ (red squares).

order 10^{-2}, values of rms fluctuations are typically of several units. No long-range organization is apparent (in particular, no dilatant shear band is observed).

A comparison of local and global frictional properties reveals a similar discrepancy, yet in the opposite direction: while friction is absent at the contact scale ($\mu_s = 0$), the material has friction ($\mu^* > 0$) at the macroscopic scale. Its origin, as in the case of spheres [19], can be ascribed to force network anisotropy. Angle θ denoting the orientation of normal directions to contacts, with respect to the x axis (flow direction), let $P(\theta)$ denote the probability density function (p.d.f.) of θ among all contacts and $\langle f_n\rangle(\theta)$ the mean normal force among contacts with orientation θ (the global average normal force is $\langle f_n\rangle$). Both functions are fitted by a similar form (as checked in Fig. 6):

$$P(\theta) = \frac{1}{2\pi}[1 + a\,\cos 2(\theta - \theta_c)], \tag{4}$$

$$\langle f_n\rangle(\theta) = \frac{\langle f_n\rangle}{2}[1 + a_n \cos 2(\theta - \theta_n)]. \tag{5}$$

For the lowest I values we measured $a \simeq 0.12$, $a_n \simeq 0.25$, while $\theta_c = \theta_n = 3\pi/4$. As previously reported [22,27,44,45], q/p is in excellent approximation expressed as

$$\frac{q}{p} = \sin\varphi = \frac{1}{2}(a + a_n). \tag{6}$$

Note that side-side contacts represent 38% of the total number of contacts, and they carry 80% of the shear stress. A more detailed study of the rheological properties of frictionless, rigid pentagons, in relation to microscopic state variables and force networks, is presented in a forthcoming publication [42].

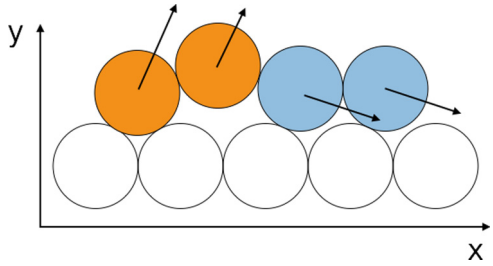

FIG. 7. (Color online) An improved schematic representation of dilatancy. As grains of the upper row, on average, flow past the bottom ones, some displacements (left; color code as in Fig. 5) increase the volume; others (right) decrease it. Friction favors the effects of the former.

To conclude we now recall the essential results of this Rapid Communication. Assemblies of rigid, frictionless polygonal particles, like disks, (i) have a finite friction angle in simple shear due to fabric and force anisotropies; but (ii) do not have any measurable dilatancy, despite side-side contacts, due to the effects of rearrangements and to the inability of configurations looser than random close packing to support static stresses. Interestingly, frictionless polygon packs exhibit a larger friction angle than disks but a similar solid fraction.

Such results stress the importance, and the seemingly counterintuitive consequences, of packing geometry and contact network instabilities in granular mechanics, which should be further investigated. The properties of frictionless grains might be correctly described by constitutive models involving numerically measured relations between stresses and microscopic variables such as coordination and fabric [46]. They are nevertheless expected to set an important constraint to first-principle approaches attempting to predict internal friction and dilatancy properties from microscopic rheophysical mechanisms [5,8,9] (see [42] for more comments).

Going back to the schematic representation of dilatancy in Fig. 1, the above findings suggest an alternative picture for dilatancy intrinsically bound to friction between particles. Namely, in a dense assembly, the intergranular friction tends to hinder compacting rearrangements more than dilating ones, thereby causing a positive global dilatancy. This picture is illustrated in Fig. 7.

J.-N. Roux's stay in Montpellier, during which this collaboration started, was supported by the MIST visiting scientist program, which is funded by the French Institut de Radioprotection et de Sûreté Nucléaire (IRSN). We are grateful to Nguyen Duc Hanh from the university Montpellier, who prepared RCP configurations of pentagons.

[1] O. Reynolds, Philos. Mag. (5th series) **20**, 469 (1885).

[2] J. D. Goddard and A. K. Didwania, Q. J. Mech. Appl. Math. **51**, 15 (1998).

[3] B. Andreotti, Y. Forterre, and O. Pouliquen, *Granular Media: Between Fluid and Solid* (Cambridge University Press, Cambridge, UK, 2013).

[4] D. M. Wood, *Soil Behaviour and Critical State Soil Mechanics* (Cambridge University Press, Cambridge, UK, 1990).

[5] S. Nemat-Nasser, J. Mech. Phys. Sol. **48**, 1541 (2000).

[6] N. P. Kruyt and L. Rothenburg, J. Stat. Mech.: Theory Exp. (2006) P07021.

[7] A. Taboada, N. Estrada, and F. Radjaï, Phys. Rev. Lett. **97**, 098302 (2006).
[8] A. Tordesillas, J. Shi, and T. Tshaikiwsky, Int. J. Numer. Anal. Meth. Geomech. **35**, 264 (2011).
[9] S. D. J. Mesarovic, J. Padbidri, and B. Muhunthan, Géotech. Lett. **2**, 61 (2012).
[10] *Discrete-Element Modeling of Granular Materials*, edited by F. Radjaï and F. Dubois (Wiley, New York, 2011).
[11] K. Iwashita and M. Oda, ASCE J. Eng. Mech. **124**, 285 (1998).
[12] N. Estrada, A. Taboada, and F. Radjaï, Phys. Rev. E **78**, 021301 (2008).
[13] J.-N. Roux, Phys. Rev. E **61**, 6802 (2000).
[14] G. Combe and J.-N. Roux, Phys. Rev. Lett. **85**, 3628 (2000).
[15] Corey S. O'Hern, L. E. Silbert, A. J. Liu, and S. R. Nagel, Phys. Rev. E **68**, 011306 (2003).
[16] A. Donev, S. Torquato, and F. H. Stillinger, Phys. Rev. E **71**, 011105 (2005).
[17] I. Agnolin and J.-N. Roux, Phys. Rev. E **76**, 061302 (2007).
[18] P.-E. Peyneau and J.-N. Roux, Phys. Rev. E **78**, 011307 (2008).
[19] P.-E. Peyneau and J.-N. Roux, Phys. Rev. E **78**, 041307 (2008).
[20] S. Torquato and F. Stillinger, Rev. Mod. Phys. **82**, 2633 (2010).
[21] C. Thornton, Géotechnique **50**, 43 (2000).
[22] E. Azéma and F. Radjaï, Phys. Rev. E **81**, 051304 (2010).
[23] B. Saint-Cyr, K. Szarf, C. Voivret, E. Azéma, V. Richefeu, J.-Y. Delenne, G. Combe, C. Nouguier-Lehon, P. Villard, P. Sornay *et al.*, Europhys. Lett. **98**, 44008 (2012).
[24] A. Donev, R. Connelly, F. H. Stillinger, and S. Torquato, Phys. Rev. E **75**, 051304 (2007).
[25] K. C. Smith, M. Alam, and T. S. Fisher, Phys. Rev. E **82**, 051304 (2010).
[26] J.-F. Camenen, Y. Descantes, and P. Richard, Phys. Rev. E **86**, 061317 (2012).
[27] E. Azéma, F. Radjaï, and F. Dubois, Phys. Rev. E **87**, 062203 (2013).
[28] A. S. J. Suiker and N. A. Fleck, ASME J. Appl. Mech. **71**, 350 (2004).
[29] T. Hatano, Phys. Rev. E **75**, 060301(R) (2007).
[30] S. Fazekas, J. Török, and J. Kertész, Phys. Rev. E **75**, 011302 (2007).
[31] F. da Cruz, S. Emam, M. Prochnow, J.-N. Roux, and F. Chevoir, Phys. Rev. E **72**, 021309 (2005).
[32] N. Estrada, E. Azéma, F. Radjaï, and A. Taboada, Phys. Rev. E **84**, 011306 (2011).
[33] M. Jean and J.-J. Moreau, in *Proceedings of the Contact Mechanics International Symposium*, edited by A. Curnier (Presses Polytechniques Universitaires Romandes, Lausanne, 1992).
[34] M. Jean, Comput. Meth. Appl. Mech. Eng. **177**, 235 (1999).
[35] F. Radjaï and V. Richefeu, Mech. Mater. **41**, 715 (2009).
[36] E. Azéma and F. Radjaï, Phys. Rev. Lett. **112**, 078001 (2014).
[37] E. Azéma and F. Radjaï, Phys. Rev. E **85**, 031303 (2012).
[38] E. Azéma, Y. Descantes, N. Roquet, J.-N. Roux, and F. Chevoir, Phys. Rev. E **86**, 031303 (2012).
[39] E. Azéma, N. Estrada, and F. Radjaï, Phys. Rev. E **86**, 041301 (2012).
[40] φ is very slightly lower, $\varphi = 10.1 \pm 0.4^\circ$, if defined via (2). The issue is discussed in [42].
[41] D. H. Nguyen, E. Azéma, F. Radjaï, and P. Sornay, Phys. Rev. E **90**, 012202 (2014).
[42] E. Azéma, J.-N. Roux, and F. Radjaï (unpublished).
[43] *Micromechanics of Granular Materials*, edited by B. Cambou, M. Jean, and F. Radjaï (Wiley-ISTE, Hoboken, NJ, 2009).
[44] L. Rothenburg and R. Bathurst, Géotechnique **39**, 601 (1989).
[45] E. Azéma, F. Radjaï, R. Peyroux, and G. Saussine, Phys. Rev. E **76**, 011301 (2007).
[46] J. Sun and S. Sundaresan, J. Fluid Mech. **682**, 590 (2011).